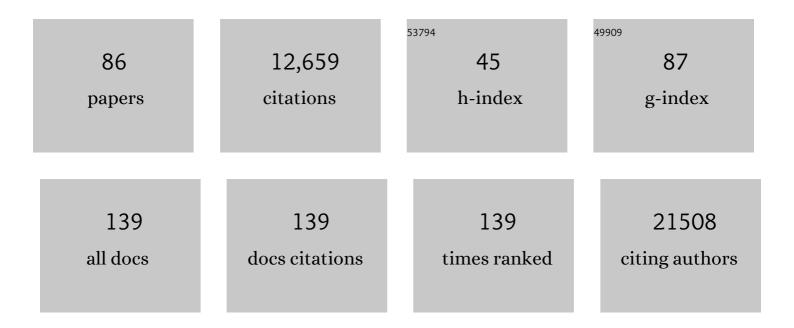
James S Fraser

List of Publications by Year in descending order

Source: https://exaly.com/author-pdf/4827885/publications.pdf Version: 2024-02-01



IAMES S EDASED

#	Article	IF	CITATIONS
1	Directed evolution of the rRNA methylating enzyme Cfr reveals molecular basis of antibiotic resistance. ELife, 2022, 11, .	6.0	10
2	Integration of software tools for integrative modeling of biomolecular systems. Journal of Structural Biology, 2022, 214, 107841.	2.8	7
3	A counter-enzyme complex regulates glutamate metabolism in Bacillus subtilis. Nature Chemical Biology, 2022, 18, 161-170.	8.0	14
4	Structural basis for context-specific inhibition of translation by oxazolidinone antibiotics. Nature Structural and Molecular Biology, 2022, 29, 162-171.	8.2	31
5	Accurate positioning of functional residues with robotics-inspired computational protein design. Proceedings of the National Academy of Sciences of the United States of America, 2022, 119, e2115480119.	7.1	6
6	Ligand binding remodels protein side-chain conformational heterogeneity. ELife, 2022, 11, .	6.0	33
7	The mechanisms of catalysis and ligand binding for the SARS-CoV-2 NSP3 macrodomain from neutron and x-ray diffraction at room temperature. Science Advances, 2022, 8, .	10.3	24
8	<scp>qFit</scp> 3: Protein and ligand multiconformer modeling for Xâ€ray crystallographic and singleâ€particle <scp>cryoâ€EM</scp> density maps. Protein Science, 2021, 30, 270-285.	7.6	34
9	Cryo-EM model validation recommendations based on outcomes of the 2019 EMDataResource challenge. Nature Methods, 2021, 18, 156-164.	19.0	73
10	ORACLE reveals a bright future to fight bacteria. ELife, 2021, 10, .	6.0	0
11	State of the structure address on MET receptor activation by HGF. Biochemical Society Transactions, 2021, 49, 645-661.	3.4	5
12	Fragment binding to the Nsp3 macrodomain of SARS-CoV-2 identified through crystallographic screening and computational docking. Science Advances, 2021, 7, .	10.3	100
13	Co-occurring Alterations in the RAS–MAPK Pathway Limit Response to MET Inhibitor Treatment in MET Exon 14 Skipping Mutation-Positive Lung Cancer. Clinical Cancer Research, 2020, 26, 439-449.	7.0	64
14	Comparative host-coronavirus protein interaction networks reveal pan-viral disease mechanisms. Science, 2020, 370, .	12.6	508
15	Discovery of allosteric binding sites by crystallographic fragment screening. Current Opinion in Structural Biology, 2020, 65, 209-216.	5.7	16
16	Synthetic group A streptogramin antibiotics that overcome Vat resistance. Nature, 2020, 586, 145-150.	27.8	63
17	Ensemble-based enzyme design can recapitulate the effects of laboratory directed evolution in silico. Nature Communications, 2020, 11, 4808.	12.8	67
18	Expanding the space of protein geometries by computational design of de novo fold families. Science, 2020, 369, 1132-1136.	12.6	57

#	Article	IF	CITATIONS
19	Genetic interaction mapping informs integrative structure determination of protein complexes. Science, 2020, 370, .	12.6	24
20	An ultrapotent synthetic nanobody neutralizes SARS-CoV-2 by stabilizing inactive Spike. Science, 2020, 370, 1473-1479.	12.6	336
21	A SARS-CoV-2 protein interaction map reveals targets for drug repurposing. Nature, 2020, 583, 459-468.	27.8	3,542
22	Assessment of the nucleotide modifications in the high-resolution cryo-electron microscopy structure of the Escherichia coli 50S subunit. Nucleic Acids Research, 2020, 48, 2723-2732.	14.5	22
23	What Will Computational Modeling Approaches Have to Say in the Era of Atomistic Cryo-EM Data?. Journal of Chemical Information and Modeling, 2020, 60, 2410-2412.	5.4	15
24	Differences in the chitinolytic activity of mammalian chitinases on soluble and insoluble substrates. Protein Science, 2020, 29, 952-963.	7.6	15
25	Assessment of enzyme active site positioning and tests of catalytic mechanisms through X-ray–derived conformational ensembles. Proceedings of the National Academy of Sciences of the United States of America, 2020, 117, 33204-33215.	7.1	39
26	Comparing serial X-ray crystallography and microcrystal electron diffraction (MicroED) as methods for routine structure determination from small macromolecular crystals. IUCrJ, 2020, 7, 306-323.	2.2	32
27	Synthetic Essentiality of Metabolic Regulator PDHK1 in PTEN-Deficient Cells and Cancers. Cell Reports, 2019, 28, 2317-2330.e8.	6.4	12
28	Temperature-jump solution X-ray scattering reveals distinct motions in a dynamic enzyme. Nature Chemistry, 2019, 11, 1058-1066.	13.6	67
29	Biomaterials in non-integer dimensions. Nature Chemistry, 2019, 11, 599-600.	13.6	5
30	Effects of \hat{I}_{\pm} -tubulin acetylation on microtubule structure and stability. Proceedings of the National Academy of Sciences of the United States of America, 2019, 116, 10366-10371.	7.1	216
31	Liquid-like and rigid-body motions in molecular-dynamics simulations of a crystalline protein. Structural Dynamics, 2019, 6, 064704.	2.3	14
32	Computational design of a modular protein sense-response system. Science, 2019, 366, 1024-1028.	12.6	91
33	Mix-and-inject XFEL crystallography reveals gated conformational dynamics during enzyme catalysis. Proceedings of the National Academy of Sciences of the United States of America, 2019, 116, 25634-25640.	7.1	56
34	A Multi-model Approach to Assessing Local and Global Cryo-EM Map Quality. Structure, 2019, 27, 344-358.e3.	3.3	55
35	Biophysical Characterization of a Disabled Double Mutant of Soybean Lipoxygenase: The "Undoing―of Precise Substrate Positioning Relative to Metal Cofactor and an Identified Dynamical Network. Journal of the American Chemical Society, 2019, 141, 1555-1567.	13.7	19
36	Bringing diffuse X-ray scattering into focus. Current Opinion in Structural Biology, 2018, 50, 109-116.	5.7	29

#	Article	IF	CITATIONS
37	Rescue of conformational dynamics in enzyme catalysis by directed evolution. Nature Communications, 2018, 9, 1314.	12.8	97
38	<i>qFit-ligand</i> Reveals Widespread Conformational Heterogeneity of Drug-Like Molecules in X-Ray Electron Density Maps. Journal of Medicinal Chemistry, 2018, 61, 11183-11198.	6.4	44
39	Extending chemical perturbations of the ubiquitin fitness landscape in a classroom setting reveals new constraints on sequence tolerance. Biology Open, 2018, 7, .	1.2	17
40	An expanded allosteric network in PTP1B by multitemperature crystallography, fragment screening, and covalent tethering. ELife, 2018, 7, .	6.0	120
41	Conformational variation of proteins at room temperature is not dominated by radiation damage. Journal of Synchrotron Radiation, 2017, 24, 73-82.	2.4	50
42	Flexibility and Design: Conformational Heterogeneity along the Evolutionary Trajectory of a Redesigned Ubiquitin. Structure, 2017, 25, 739-749.e3.	3.3	22
43	Cytidine deaminase efficiency of the lentiviral viral restriction factor APOBEC3C correlates with dimerization. Nucleic Acids Research, 2017, 45, 3378-3394.	14.5	38
44	Hydrogen–Deuterium Exchange of Lipoxygenase Uncovers a Relationship between Distal, Solvent Exposed Protein Motions and the Thermal Activation Barrier for Catalytic Proton-Coupled Electron Tunneling. ACS Central Science, 2017, 3, 570-579.	11.3	55
45	XFEL structures of the influenza M2 proton channel: Room temperature water networks and insights into proton conduction. Proceedings of the National Academy of Sciences of the United States of America, 2017, 114, 13357-13362.	7.1	64
46	Allosteric Inhibitors, Crystallography, and Comparative Analysis Reveal Network of Coordinated Movement across Human Herpesvirus Proteases. Journal of the American Chemical Society, 2017, 139, 11650-11653.	13.7	13
47	Measuring and modeling diffuse scattering in protein X-ray crystallography. Proceedings of the National Academy of Sciences of the United States of America, 2016, 113, 4069-4074.	7.1	48
48	Preprints for the life sciences. Science, 2016, 352, 899-901.	12.6	119
49	Data publication with the structural biology data grid supports live analysis. Nature Communications, 2016, 7, 10882.	12.8	113
50	High-density grids for efficient data collection from multiple crystals. Acta Crystallographica Section D: Structural Biology, 2016, 72, 2-11.	2.3	62
51	CryptoSite: Expanding the Druggable Proteome by Characterization and Prediction of Cryptic Binding Sites. Journal of Molecular Biology, 2016, 428, 709-719.	4.2	190
52	Determination of ubiquitin fitness landscapes under different chemical stresses in a classroom setting. ELife, 2016, 5, .	6.0	71
53	Automated structure refinement of macromolecular assemblies from cryo-EM maps using Rosetta. ELife, 2016, 5, .	6.0	407
54	One Crystal, Two Temperatures: Cryocooling Penalties Alter Ligand Binding to Transient Protein Sites. ChemBioChem, 2015, 16, 1560-1564.	2.6	76

#	Article	IF	CITATIONS
55	Predicting X-ray diffuse scattering from translation–libration–screw structural ensembles. Acta Crystallographica Section D: Biological Crystallography, 2015, 71, 1657-1667.	2.5	14
56	Exposing Hidden Alternative Backbone Conformations in X-ray Crystallography Using qFit. PLoS Computational Biology, 2015, 11, e1004507.	3.2	81
57	Negative Epistasis and Evolvability in TEM-1 β-Lactamase—The Thin Line between an Enzyme's Conformational Freedom and Disorder. Journal of Molecular Biology, 2015, 427, 2396-2409.	4.2	102
58	High-resolution structures of the M2 channel from influenza A virus reveal dynamic pathways for proton stabilization and transduction. Proceedings of the National Academy of Sciences of the United States of America, 2015, 112, 14260-14265.	7.1	92
59	Integrative, dynamic structural biology at atomic resolution—it's about time. Nature Methods, 2015, 12, 307-318.	19.0	220
60	Lineage-Specific Viral Hijacking of Non-canonical E3ÂUbiquitin Ligase Cofactors in the Evolution of Vif Anti-APOBEC3 Activity. Cell Reports, 2015, 11, 1236-1250.	6.4	42
61	EMRinger: side chain–directed model and map validation for 3D cryo-electron microscopy. Nature Methods, 2015, 12, 943-946.	19.0	799
62	Keep on Moving: Discovering and Perturbing the Conformational Dynamics of Enzymes. Accounts of Chemical Research, 2015, 48, 423-430.	15.6	84
63	From deep TLS validation to ensembles of atomic models built from elemental motions. Acta Crystallographica Section D: Biological Crystallography, 2015, 71, 1668-1683.	2.5	14
64	Mapping the conformational landscape of a dynamic enzyme by multitemperature and XFEL crystallography. ELife, 2015, 4, .	6.0	143
65	Conformational dynamics of a crystalline protein from microsecond-scale molecular dynamics simulations and diffuse X-ray scattering. Proceedings of the National Academy of Sciences of the United States of America, 2014, 111, 17887-17892.	7.1	55
66	Incorporation of protein flexibility and conformational energy penalties in docking screens to improve ligand discovery. Nature Chemistry, 2014, 6, 575-583.	13.6	124
67	Protein structural ensembles are revealed by redefining X-ray electron density noise. Proceedings of the United States of America, 2014, 111, 237-242.	7.1	79
68	Integrated description of protein dynamics from room-temperature X-ray crystallography and NMR. Proceedings of the National Academy of Sciences of the United States of America, 2014, 111, E445-54.	7.1	142
69	E pluribus unum, no more: from one crystal, many conformations. Current Opinion in Structural Biology, 2014, 28, 56-62.	5.7	53
70	Discovery and Characterization of Gut Microbiota Decarboxylases that Can Produce the Neurotransmitter Tryptamine. Cell Host and Microbe, 2014, 16, 495-503.	11.0	473
71	Crystal Cryocooling Distorts Conformational Heterogeneity in a Model Michaelis Complex of DHFR. Structure, 2014, 22, 899-910.	3.3	131
72	Automated identification of functional dynamic contact networks from X-ray crystallography. Nature Methods, 2013, 10, 896-902.	19.0	130

#	Article	IF	CITATIONS
73	From Structure to Systems: High-Resolution, Quantitative Genetic Analysis of RNA Polymerase II. Cell, 2013, 154, 775-788.	28.9	132
74	Flexible Backbone Sampling Methods to Model and Design Protein Alternative Conformations. Methods in Enzymology, 2013, 523, 61-85.	1.0	44
75	From Systems to Structure: Bridging Networks and Mechanism. Molecular Cell, 2013, 49, 222-231.	9.7	46
76	Control of protein signaling using a computationally designed GTPase/GEF orthogonal pair. Proceedings of the National Academy of Sciences of the United States of America, 2012, 109, 5277-5282.	7.1	73
77	CheShift-2 resolves a local inconsistency between two X-ray crystal structures. Journal of Biomolecular NMR, 2012, 54, 193-198.	2.8	4
78	Systematic Functional Prioritization of Protein Posttranslational Modifications. Cell, 2012, 150, 413-425.	28.9	375
79	Mining electron density for functionally relevant protein polysterism in crystal structures. Cellular and Molecular Life Sciences, 2011, 68, 1829-1841.	5.4	23
80	Accessing protein conformational ensembles using room-temperature X-ray crystallography. Proceedings of the National Academy of Sciences of the United States of America, 2011, 108, 16247-16252.	7.1	511
81	Automated electronâ€density sampling reveals widespread conformational polymorphism in proteins. Protein Science, 2010, 19, 1420-1431.	7.6	155
82	The tumor-associated EpCAM regulates morphogenetic movements through intracellular signaling. Journal of Cell Biology, 2010, 191, 645-659.	5.2	58
83	Hidden alternative structures of proline isomerase essential for catalysis. Nature, 2009, 462, 669-673.	27.8	447
84	Immunoglobulin-like domains on bacteriophage: weapons of modest damage?. Current Opinion in Microbiology, 2007, 10, 382-387.	5.1	86
85	An atypical receiver domain controls the dynamic polar localization of the Myxococcus xanthus social motility protein FrzS. Molecular Microbiology, 2007, 65, 319-332.	2.5	32
86	lg-Like Domains on Bacteriophages: A Tale of Promiscuity and Deceit. Journal of Molecular Biology, 2006, 359, 496-507.	4.2	169